Sholl analysis: a quantitative comparison of semi-automated methods

Research article

Kate E Binley[a], Wai S Ng[a], James R Tribble[a], Bing Song[b], James E Morgan[a] *

a) School of Optometry and Vision Sciences, Cardiff University, Maindy Road, Cardiff, CF24 4LU, Wales, United Kingdom

b) School of Dentistry, Cardiff University, Heath Park, Cardiff, CF14 4XY, Wales, United Kingdom

Pages: 22 (including figures)

Figures: 4

Word count: 4503

Funding: Biotechnology and Biological Sciences Research Council (UK)

* Corresponding author. Tel.: +44 29 2074 3222
E-mail address: MorganJE3@cf.ac.uk (J.E. Morgan)
Address: School of Optometry and Vision Sciences
Cardiff University
Maindy Road
Cardiff
CF24 4LU
Wales
United Kingdom

Highlights

- We compare four Sholl analysis methods to the manual method.
- We validate two Sholl analysis methods.
- We highlight two errors in two Sholl analysis methods.

Abstract

Background: Sholl analysis remains one of the most commonly used methods to quantify neuronal dendritic complexity and is therefore a key analysis tool in neurobiology. While initially proposed when the quantification of neuronal structure was undertaken manually, the advent of software packages allowing automated analysis has resulted in the introduction of several semi and fully automated methods to quantify dendritic complexity. Unfortunately results from these methods have not in all cases been consistent. We therefore compared the results of five commonly used methods (Simple Neurite Tracer, manual, Fast Sholl, Bitmap, and Ghosh lab) using manual analysis as a ground truth.

New Method: Comparison of four semi-automated methods to the manual method using diolistically labelled mouse retinal ganglion cells.

Results: We report consistency across a range of published techniques. While the majority perform well (Simple Neurite Tracer and Fast Sholl profiles have areas under the curve within 4.5% of the profile derived using the manual method), we highlight two areas in two of the methods (Bitmap and Ghosh lab methods) where errors may occur, namely undercounting (>20% relative to the manual profile) and a second peak.

Comparison with Existing Methods: Our results support published validation of the Fast Sholl method.

Conclusions: Our study highlights the importance of manual calibration of automated analysis software.

Keywords: Sholl analysis; Dendritic pruning; Automated analysis.

1. Introduction

Sholl analysis (Sholl, 1953), is a widely used method in neurobiology to quantify the complexity of dendritic arbours. A Sholl profile is obtained by plotting the number of dendrite intersections against the radial distance from the soma centre. The number of intersections is then plotted as a function of radial distance from which a summary estimate (area under the Sholl profile) can be derived as a single measure of dendritic complexity. Assessing neuronal morphology changes is essential when investigating mechanisms involved in disease progression and treatments in animal models (Gutierrez et al., 2004; Torres-Garcia et al., 2012). Sholl plots can also be used to summarise the distribution of synaptic contacts or mitochondria within dendritic arbours and provide a sensitive read out for neuronal development and disease (Barrow et al., 1999; Beauquis et al., 2013; Eyermann et al., 2012; Isaura Martinez-Tellez et al., 2009; Lerner et al., 2012; Schoenen, 1982; Williams et al., 2012). Sholl analysis is an invaluable tool for studying mechanisms of disease, as well as quantifying the effects of potential treatments, such as neurotrophic support (Rekha et al., 2011). Right- and left-ward shifts of the Sholl profile are indicative of neuron health and profile peak amplitude provides an index for the complexity of the dendritic arbour (Gavalda et al., 2009; Williams et al., 2013). Further, analysing the branching pattern will help establish the cell type. Number of branches, number of dendrites, and dendritic field size are among the 15 parameters outlined in the Chalupa classification system of mouse retinal ganglion cells (RGCs) (Coombs et al., 2006).

Most Sholl analysis packages use 2D tracing of the cell therefore the analysis is carried out in 2D. This may provide relatively accurate measurements for RGCs, which have planar stratification of dendrites (Cook and Podugolnikova, 2001), however in studies using non-planar neurons a 2D Sholl analysis may introduce error - in these cases 3D analysis may be more appropriate. A 3D reconstruction of a neuron can be created using the Neurolucida dendrite package.

Manual Sholl analysis is a time consuming constraint on the number of cells which can be analysed. To address this, several groups have developed methods to semi-automate the neuron tracing and perform Sholl counts available as open-source Java plugins and MATLAB scripts (Gensel et al., 2010; Meijering et al., 2004; Myatt et al., 2012; Peng et al., 2011; Schmitz et al., 2011; Zhao et al., 2011).

Sholl analysis methods generate concentric rings radiating from the soma centre and at each ring the number of dendrites is counted based on difference in contrast between the arbour and the background. The Fast Sholl method uses a novel algorithm which takes the primary dendrite start points, dendritic branch points and dendritic termination points to predict how many dendrites are located at each point of radial distance (Gutierrez and Davies, 2007). The main limitation of this method is that it assumes that all the dendrites grow away from the soma, i.e. terminate distally to the branch point. The termination points of dendrites which curve back towards the soma may therefore be counted before the respective branch points, resulting in undercounting (Gutierrez and Davies, 2007).

Although some validations are available, for example for the Fast Sholl MATLAB script (Gutierrez and Davies, 2007) and the Bonfire MATLAB script (Langhammer et al., 2010), the independent validation of these techniques has not been undertaken in a systematic manner and no comparisons have been made independently between techniques. We therefore evaluated four most commonly used and available techniques (three Java plugins and one MATLAB script) against the manual method.

2. Methods

2.1 Cell Labelling and Image Acquisition

Adult mice were sacrificed by cervical dislocation in accordance with the regulations of the UK Home Office. Eyes were immediately enucleated and retinas gently dissected in Neurobasal-A culture medium (Gibco, Paisley, UK) with the RGC layer facing up on 0.4 µm PTFE cell culture inserts (Millipore, Watford, UK). The inserts were placed into culture dishes (Millipore) containing 1.2 mL of Neurobasal-A culture medium. DiI and DiO-coated tungsten bullets were prepared using 3 mg DiI, 6 mg DiO and 200 mg tungsten beads (1.7 µm diameter) (Grutzendler et al., 2003). The cells were labelled with the DiI/DiO labelled tungsten particles using a Helios gene gun (Bio-Rad, Hertfordshire, UK), fired at 100 psi helium 5 cm from the retina. The beads were fired through a 3 µm PET membrane filter (Scientific Laboratory Supplies Ltd., Yorkshire, UK) to prevent particle clumping and excessive labelling. The explants were then incubated for 30 minutes at 37°C, 5% CO_2. The tissue was fixed in 4% PFA and the nuclear stain TO-PRO-3 (Invitrogen Ltd., Paisley, UK) was applied to identify the RGC layer. Finally, the explants were coverslipped with Prolong Gold antifade reagent (Invitrogen Ltd.).

Images of fluorescently labelled RGCs (Fig. 1A) were obtained by confocal microscopy (Zeiss, LSM 510, release version 4.2 SP1). A separate channel was used for each of the dyes and a 3D image was acquired by creating a z-stack in 1 µm steps. The acquired images were split into single channels using Fiji (Schindelin et al., 2012) and stored as 8-bit images.

2.2 Sholl Analysis

Images of labelled cells were imported into Fiji and traced without z-projecting the stacks by two observers using the semi-automated plugin Simple Neurite Tracer (Longair et al., 2011, version 2.02). Sholl analyses were then carried out independently by three observers. Two observers traced

approximately 50% of the cells each which were then analysed using all methods (except Fast Sholl) on the cells they had traced. The third observer carried out all Fast Sholl analysis using information on soma centre provided by the first two observers. The same location to mark the soma centre was used for each method.

Sholl analysis was performed using Simple Neurite Tracer by first extending the longest primary dendrite to the soma centre. The non-extended tracing was used to produce a z-projected 8-bit trace image (Fig. 1B), which was used to carry out the additional four methods of Sholl analysis. The estimated geometric centre was marked using the point tool in Fiji and the image was analysed with the Fiji plugins Bitmap Sholl Analysis (http://fiji.sc/Sholl_Analysis, version 3.1) and Ghosh lab Sholl Analysis (http://labs.biology.ucsd.edu/ghosh/software/, version 1.0). For the Fast Sholl MATLAB (2009 version) method (scripts from Davies and Gutierrez (Gutierrez and Davies, 2007)) the soma centre, dendrite branch points and dendrite termination points were marked on the image prior to analysis. The manual method was carried out by digitally tracing rings centred at the soma centre and intersections counted (Fig. 1C). All Sholl analyses were carried out at 10 µm intervals to a maximum radius of 500 µm.

2.3 Statistical Analysis

Microsoft Excel (Office 2010) was used for data formatting and statistical analysis was carried out using IBM SPSS statistics (version 20). Total area under the curve (AUC) was calculated using the trapezoidal rule for each Sholl profile and expressed as a percentage of the AUC of the manual method profile. AUC generates a single measure of the Sholl profile and is therefore a useful single metric to compare overall Sholl profiles. Inter-rater reliability of the manual technique was assessed with an intraclass correlation coefficient (ICC) test using a two-way mixed effects model and 95% confidence intervals measuring absolute agreement between intersections at 10 µm radial intervals

for 12 cells measured by two observers (Bartko, 1966). The same model was used to test the agreement between each method and the manual method. Comparison of agreement between methods was analysed with Bland-Altman plots (Bland and Altman, 1986) in which the total number of intersections for each cell with the manual method was compared to the total number of intersections for each cell with each of the other methods.

2.4 Image processing and code editing

Sholl analysis was carried out on a sub-set of cells using the Ghosh lab and Bitmap methods. The Bitmap plugin advises the use of direct bitmap images and the Ghosh lab plugin was originally written to enable analysis of tracings, however since both plugins are derived from the same 2D algorithm the potential confounding effects of prior image processing should be considered. To do this, each cell was analysed using both a rasterised 8-bit tracing image and a direct bitmap image (i.e. a thresholded 8-bit image). In addition, blank images were analysed using both methods using the same centre points as each cell, and readings obtained from this analysis were subtracted from the tracing analysis. Finally, cell tracings were analysed using an edited version of the Ghosh lab code, whereby the number of groups on line 445 of the code was reduced from 1.5 to 1. This section of the code helps to differentiate between two dendrites by assigning points of each dendrite to different groups.

3. Results

Comparison of the four Sholl analysis methods was carried out against the manual method as the ground truth. 62 cells labelled with DiI and DiO were traced by two observers using Simple Neurite Tracer. Inter-observer agreement for the manual analysis was almost perfect (ICC range = 0.883-0.976). Time estimates for each analysis technique (per cell) are as follows: tracing using Simple Neurite Tracer 30 minutes, manual and Fast Sholl 5 minutes, Bitmap and Ghosh lab 1 minute, Simple Neurite Tracer less than 10 seconds.

The Sholl profiles of cell tracings are shown in Fig. 2. The Sholl profiles obtained by Simple Neurite Tracer analysis (Fig. 2A) were almost identical to those obtained by manual method (Fig. 2B). Similarly, the Fast Sholl curve (Fig. 2C) has showed a close match with the manual method curve, although the amplitude of the peak is slightly lower and the curve does not begin at zero. To describe agreement with the manual method over the first 300 µm an ICC test using a two-way mixed effects model was performed and generated ICCs of 0.998 and 0.959 for Simple Neurite Tracer and Fast Sholl, respectively. The Sholl profile AUC differences over the first 200 µm relative to the manual method for Simple Neurite Tracer and Fast Sholl are +4.5% and -3.5%, respectively. By contrast, both the Bitmap Sholl analysis and Ghosh Sholl Analysis profiles have reduced main peak amplitude of >5 intersections compared to the manual method profile, and a second, lower peak to the right (Fig.s 2D-E). ICCs for the Bitmap and Ghosh lab methods are 0.859 and 0.863, respectively, relative to the manual method over the first 300 µm. The Sholl profile AUCs for Bitmap and Ghosh lab Sholl analyses are 21% and 23%, respectively, smaller than the AUC for the manual method (over the first 200 µm).

Bland-Altman plots were constructed (Fig.s 3A-D) using total intersection values for each cell to determine the presence of any systematic errors in the Sholl counts as a function of radial distance. Simple Neurite Tracer (Fig. 3A, limits of agreement 38.4) and Fast Sholl (Fig. 3B, limits of agreement 77.3) produce measurements which vary very little from the manual method. By contrast, Bitmap

Sholl Analysis (Fig. 3C) and Ghosh lab Sholl Analysis (Fig. 3D) produce data which vary greatly to readings obtained with the manual method (limits of agreement are 98.7 and 103, respectively).

A sub-set of cells (n=10) was analysed with the Ghosh lab and Bitmap methods in order to identify the source of error in both methods. Analysis was compared to data from the manual method for the same 10 cells (Fig. 4A). To investigate the effects of image processing the cells were first analysed with both methods using tracing (rasterised) images (Fig.s 4B-C), and then with direct bitmap images (Fig.s 4D-E). Relative to the manual method, analysis of both types of image using Ghosh lab and Bitmap methods produced undercounting and an artefact at approximately 250 µm, however undercounting was much greater with Ghosh lab analysis of direct bitmap images. It was noted that analysis of direct bitmap images generated greater error bars than analysis of tracing images.

To account for any artefacts produced by Fiji, readings obtained from analysis of blank images were subtracted from readings obtained by analysis of tracing images (Fig.s 4F-G). This subtraction resulted in slight undercounting relative to the non-subtracted Sholl profiles (i.e. tracing image analysis), and removal of the second peak.

Finally, the 10 cells were analysed with an edited version of the Ghosh lab code to determine the effect of altering the grouping threshold (Fig. 4H). The code amendment resulted in overcounting relative to the manual method and presence of the same artefact to the right of the main peak.

4. Discussion

We compared four commonly used Sholl analysis techniques to the manual method. Sholl profiles produced by Simple Neurite Tracer and Fast Sholl Analysis showed excellent agreement with manual Sholls. It should be noted that the presence of large errors bars in Fig.s 2A-E is a result of pooling multiple classes of RGC, which each have their own distinct Sholl profile (Coombs et al., 2006). Simple Neurite Tracer shows good agreement with the manual method for the total number of intersections (Fig. 3A). The Gutierrez model assumes that the termination point of each dendrite is the most distal point of the dendrite raising the possibility that this method could undercount the number of intersections if dendrites curved back towards the soma, a situation highlighted by the authors (Gutierrez and Davies, 2007). The relevance of this area varies with the test neuronal population. For example, with RGCs such as B- and D-type RGCs (Sun et al., 2002). Additionally, analysis of cells with small somas may generate further error, since branching before the first 10 µm ring could be missed. The non-zero start to the Fast Sholl curve may be explained by the fact that this technique uses the number of primary dendrites indicated by the user as the starting value. This is likely to produce more error when analysing neurons with large soma diameters. Despite this, Fast Sholl shows only a small amount of variation from the manual method (Fig. 3B).

Simple Neurite Tracer may provide a solution to the aforementioned issue with analysing non-planar cells in 2D since Simple Neurite Tracer Sholl analysis is carried out using tracings which are not z-projected. Further errors in the Ghosh lab and Bitmap methods may therefore be masked somewhat in this study, which uses relatively planar RGCs.

Bitmap Sholl Analysis and Ghosh lab Sholl Analysis show significant undercounting (>20% over the first 200 µm) (Fig.s 2D-E). Inaccuracies at the far right of the curve, indicated by a second peak, could generate misleading data in studies using dendritic pruning as a measure of cell health. Statistical analysis of the data supports the inaccuracies with Bitmap and Ghosh lab methods by demonstrating large percentage differences relative to the manual method. Bland-Altman plots suggest the

presence of systematic errors, indicated by large limits of agreement, relative to the manual method, and the sporadic arrangement of data points in Fig.s 3C-D.

Comparison of image processing effects for Bitmap and Ghosh lab analyses suggests that although rasterisation of the image reduces clarity, use of a tracing image increases reproducibility. In addition, using the same type of image for all methods enables comparisons between methods to be made more confidently. Large undercounting using Ghosh lab analysis of direct bitmap images is likely due to the fact that this algorithm is designed to be used with cell tracings. It was noted that with the direct analysis of bitmap images, overcounting was noted with more densely branched cells and over-stained cells; undercounting was associated with more sparsely branched cells and poorly stained cells. These observations are consistent with the large error bars with analysis of this type of image. Image processing comparison highlights the overall benefit of a semi-automated tracing method. Although the Bitmap method is designed to remove the need for cell tracing, manual input reduces error introduced by overlapping cells and background fluorescence, which are common confounders with many staining techniques. Furthermore, Simple Neurite Tracer allows the user to scroll through slices in the z-plane and follow individual dendrites to ensure tracing, and therefore analysis, is more accurate. Simple Neurite Tracer, in addition to its accuracy, is the most usable Sholl analysis method to use for traced images.

Subtraction of readings obtained from a blank image using Ghosh lab and Bitmap analysis on a sub-set of removed the second peak. Fiji creates a rectangular boundary on the bitmap canvas, resulting in generation of an artefact in the Sholl profile. It is suggested that in order to remove this problem the analyses should be additionally run on blank images, as shown here, or the canvas size for each image increased so that the image outline does not interfere with readings.

Analysis of the Ghosh lab code indicates that errors may be generated by the value of the group count assigned on code line 445. The relationship between this fixed value and the Sholl count is unclear since correction to a group count of 1.0 resulted in an overestimation of dendrite

complexity. It is suggested that the algorithms for Ghosh lab and Bitmap analyses be revised to remove the problem of undercounting. Importantly, Fiji is linked to GitHub (https://github.com/fiji), which allows rapid updating and code review, therefore bugs can be identified and following the fix all users will be updated with the correctly functioning version of each plugin. Unfortunately the limitation with using pixel boundary detection models, such as Bitmap and Ghosh lab, is that they are prone to errors. For example, if the image pixels and the boundary pixels are exactly perpendicular at the point of intersection the image pixels will not be detected, resulting in undercounting. Consequently, a better method would be to use a mathematical model, which defines the coordinates of each locus, thereby providing more accurate analysis.

In conclusion, this study validates the Simple Neurite Tracer Fiji plugin and supports the published validation of the Fast Sholl MATLAB script. We suggest amendments to the algorithms of the Fiji plugins Bitmap Sholl Analysis and Ghosh lab Sholl Analysis to remove the issue of undercounting. We propose that the artefacts to the right of the main peak may be due to generation of an image outline by Fiji rather than a bug in the plugin codes, and recommend the application of mathematical models for this type of analysis in the future. Our results highlight the importance of validation of automated techniques against the manual method, particularly in situations where remodelling of the dendritic arbours could occur, which might generate atypical configurations.

Acknowledgements

This work was supported by a postgraduate studentship funded in part by the Biotechnology and Biological Sciences Research Council (UK).

The authors are extremely grateful to Hannah Jones and David Rogers for scrupulously checking the code for possible sources of error.

References

Barrow PA, Holmgren CD, Tapper AJ, Jefferys JGR. Intrinsic physiological and morphological properties of principal cells of the hippocampus and neocortex in hamsters infected with scrapie. Neurobiology of Disease, 1999; 6: 406-23.

Bartko JJ. The intraclass correlation coefficient as a measure of reliability. Psychol Rep, 1966; 19: 3-11.

Beauquis J, Pavia P, Pomilio C, Vinuesa A, Podlutskaya N, Galvan V, Saravia F. Environmental enrichment prevents astroglial pathological changes in the hippocampus of APP transgenic mice, model of Alzheimer's disease. Exp Neurol, 2013; 239: 28-37.

Bland JM, Altman DG. Statistical methods for assessing agreement between two methods of clinical measurement. Lancet, 1986; 1: 307-10.

Cook JE, Podugolnikova TA. Evidence for spatial regularity among retinal ganglion cells that project to the accessory optic system in a frog, a reptile, a bird, and a mammal. Vis Neurosci, 2001; 18: 289-97.

Coombs J, van der List D, Wang GY, Chalupa LM. Morphological properties of mouse retinal ganglion cells. Neuroscience, 2006; 140: 123-36.

Eyermann C, Czaplinski K, Colognato H. Dystroglycan promotes filopodial formation and process branching in differentiating oligodendroglia. J Neurochem, 2012; 120: 928-47.

Gavalda N, Gutierrez H, Davies AM. Developmental switch in NF-kappaB signalling required for neurite growth. Development, 2009; 136: 3405-12.

Gensel JC, Schonberg DL, Alexander JK, McTigue DM, Popovich PG. Semi-automated Sholl analysis for quantifying changes in growth and differentiation of neurons and glia. J Neurosci Methods. 2010 Elsevier B.V: Netherlands, 2010: 71-9.

Grutzendler J, Tsai J, Gan WB. Rapid labeling of neuronal populations by ballistic delivery of fluorescent dyes. Methods, 2003; 30: 79-85.

Gutierrez H, Davies AM. A fast and accurate procedure for deriving the Sholl profile in quantitative studies of neuronal morphology. J Neurosci Methods: Netherlands, 2007: 24-30.

Gutierrez H, Dolcet X, Tolcos M, Davies A. HGF regulates the development of cortical pyramidal dendrites. Development: England, 2004: 3717-26.

Isaura Martinez-Tellez R, Hernandez-Torres E, Gamboa C, Flores G. Prenatal Stress Alters Spine Density and Dendritic Length of Nucleus Accumbens and Hippocampus Neurons in Rat Offspring. Synapse, 2009; 63: 794-804.

Langhammer CG, Previtera ML, Sweet ES, Sran SS, Chen M, Firestein BL. Automated Sholl analysis of digitized neuronal morphology at multiple scales: Whole cell Sholl analysis versus Sholl analysis of arbor subregions. Cytometry A, 2010; 77: 1160-8.

Lerner RP, Martinez L, Zhu CN, Chesselet MF, Hickey MA. Striatal atrophy and dendritic alterations in a knock-in mouse model of Huntington's disease. Brain Research Bulletin, 2012; 87: 571-8.

Longair MH, Baker DA, Armstrong JD. Simple Neurite Tracer: open source software for reconstruction, visualization and analysis of neuronal processes. Bioinformatics, 2011; 27: 2453-4.

Meijering E, Jacob M, Sarria JCF, Steiner P, Hirling H, Unser M. Design and validation of a tool for neurite tracing and analysis in fluorescence microscopy images. Cytometry Part A, 2004; 58A: 167-76.

Myatt DR, Hadlington T, Ascoli GA, Nasuto SJ. Neuromantic - from semi-manual to semi-automatic reconstruction of neuron morphology. Front Neuroinform, 2012; 6: 4.

Peng H, Long F, Myers G. Automatic 3D neuron tracing using all-path pruning. Bioinformatics, 2011; 27: i239-47.

Rekha J, Veena LR, Prem N, Kalaivani P, Choudhury R, Alladi PA, Agrahari M, Raju TR, Kutty BM. NIH-3T3 fibroblast transplants enhance host regeneration and improve spatial learning in ventral subicular lesioned rats. Behav Brain Res. 2010 Elsevier B.V: Netherlands, 2011: 315-24.

Schindelin J, Arganda-Carreras I, Frise E, Kaynig V, Longair M, Pietzsch T, Preibisch S, Rueden C, Saalfeld S, Schmid B, Tinevez JY, White DJ, Hartenstein V, Eliceiri K, Tomancak P, Cardona A. Fiji: an open-source platform for biological-image analysis. Nat Methods, 2012; 9: 676-82.

Schmitz SK, Hjorth JJ, Joemai RM, Wijntjes R, Eijgenraam S, de Bruijn P, Georgiou C, de Jong AP, van Ooyen A, Verhage M, Cornelisse LN, Toonen RF, Veldkamp WJ. Automated analysis of neuronal morphology, synapse number and synaptic recruitment. J Neurosci Methods, 2011; 195: 185-93.

Schoenen J. The dendritic organization of the human spinal-cord - the dorsal horn. Neuroscience, 1982; 7: 2057-87.

Sholl DA. Dendritic organization in the neurons of the visual and motor cortices of the cat. Journal of Anatomy, 1953; 87: 387-&.

Sun WZ, Li N, He SG. Large-scale morphological survey of mouse retinal ganglion cells. Journal of Comparative Neurology, 2002; 451: 115-26.

Torres-Garcia ME, Solis O, Patricio A, Rodriguez-Moreno A, Camacho-Abrego I, Limon ID, Flores G. Dendritic morphology changes in neurons from the prefrontal cortex, hippocampus and nucleus accumbens in rats after lesion of the thalamic reticular nucleus. Neuroscience, 2012; 223: 429-38.

Williams PA, Piechota M, von Ruhland C, Taylor E, Morgan JE, Votruba M. Opa1 is essential for retinal ganglion cell synaptic architecture and connectivity. Brain: England, 2012: 493-505.

Williams PA, Thirgood RA, Oliphant H, Frizzati A, Littlewood E, Votruba M, Good MA, Williams J, Morgan JE. Retinal ganglion cell dendritic degeneration in a mouse model of Alzheimer's disease. Neurobiol Aging, 2013; 34: 1799-806.

Zhao T, Xie J, Amat F, Clack N, Ahammad P, Peng H, Long F, Myers E. Automated reconstruction of neuronal morphology based on local geometrical and global structural models. Neuroinformatics, 2011; 9: 247-61.

Web references

http://fiji.sc/Sholl_Analysis. Date last accessed: 26/07/13.

http://labs.biology.ucsd.edu/ghosh/software/. Date last accessed: 26/07/13.

https://github.com/fiji. Date last accessed: 01/10/13.

Figures and legends

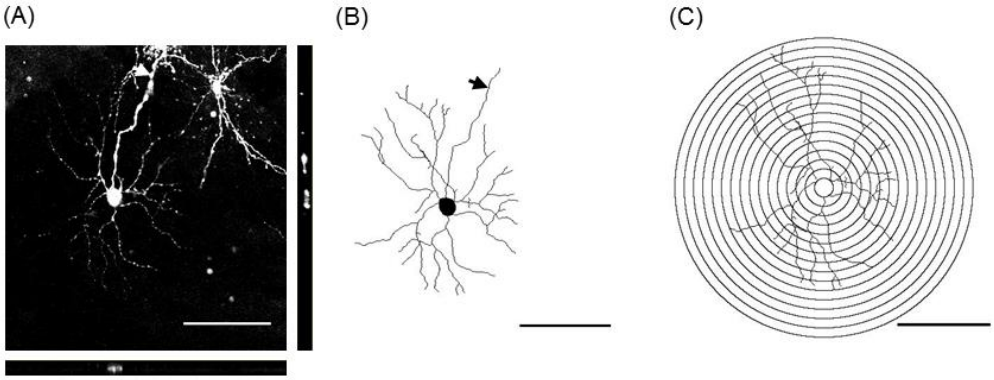

Fig. 1. Mouse RGC labelled with DiI and DiO. (A) Projected z-stack image with orthogonal views. (B) 8-bit tracing constructed using the Fiji plugin Simple Neurite Tracer. The axon and soma were drawn post-analysis. (C) 8-bit tracing with digitally applied concentric rings spaced 10 µm apart centred on the soma centre. This image was used to count the number of intersections for the manual Sholl analysis technique. Scale bar: 100 µm. Axons indicated by arrows.

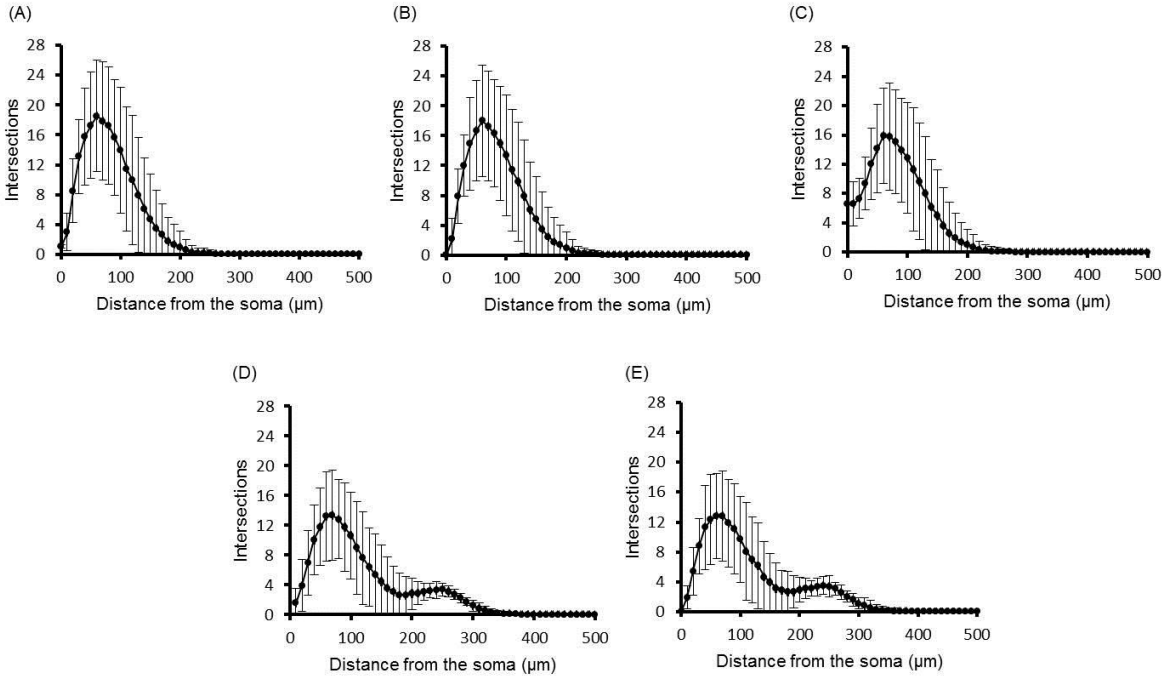

Fig. 2. Sholl profiles for each method for 62 cells. Intersections were counted at 10 µm intervals from the soma centre to a radius of 500 µm. (A) Simple Neurite Tracer. (B) Manual method. (C) Fast Sholl. (D) Bitmap Sholl Analysis. (E) Ghosh lab Sholl Analysis. Curves represent mean intersection values ±SD.

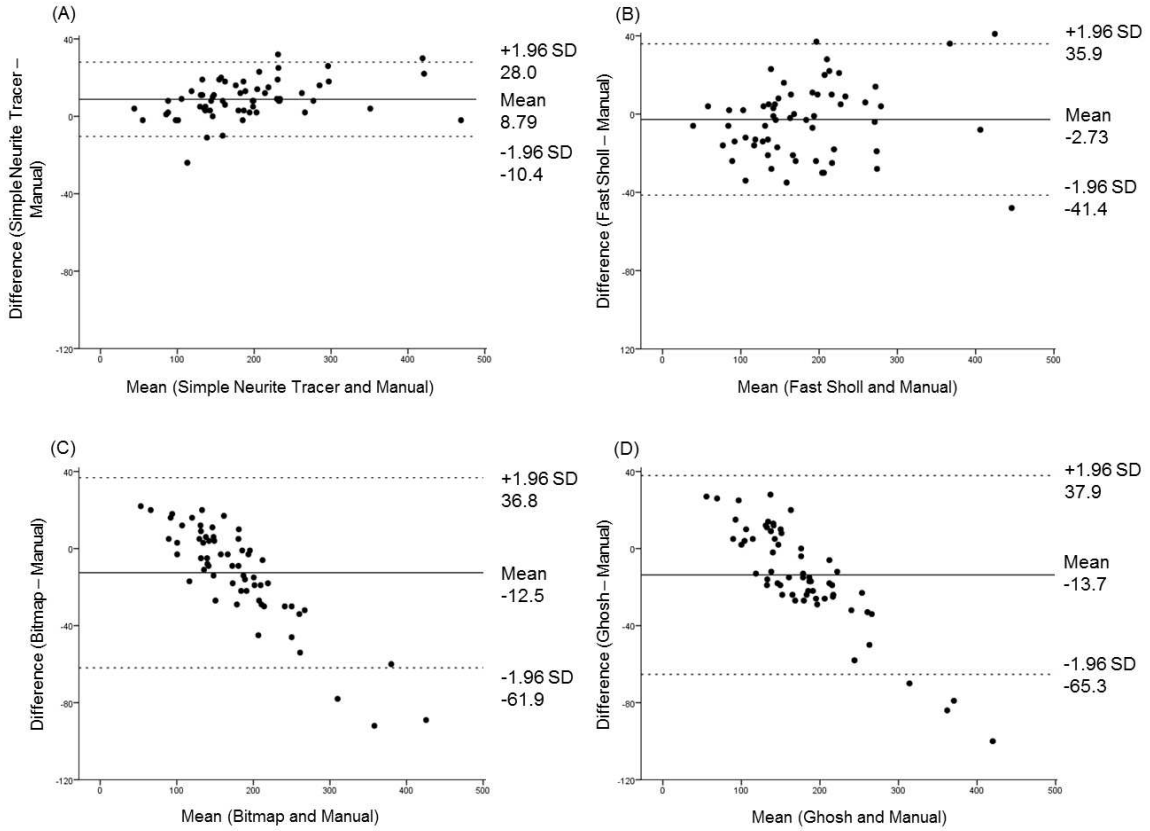

Fig. 3. Bland-Altman plots comparing total intersections for each method against the manual method for 62 cells. In each case the difference in total number of intersections between each method for each cell is plotted against the average number of total intersections for the two methods for each cell. The average difference between the two methods for all cells and the limits of agreement are indicated on each plot. (A) Simple Neurite Tracer. (B) Fast Sholl. (C) Bitmap Sholl Analysis. (D) Ghosh lab Sholl Analysis.

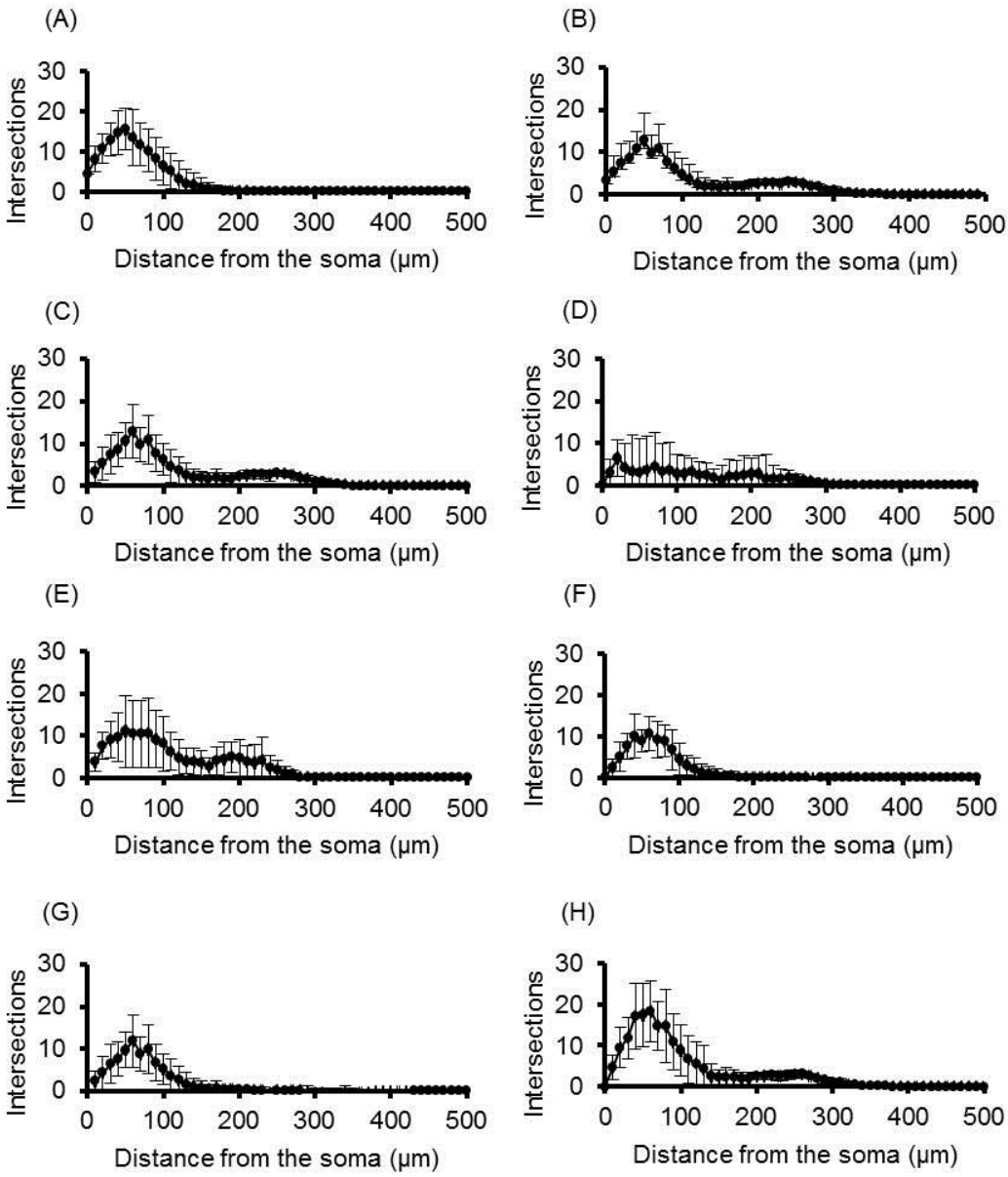

Fig. 4. Sholl profiles for 10 cells to compare the effect of image processing, potential image artefacts, and code editing. Dendrite intersections were counted at 10 µm intervals to a radius of 500 µm. (A) Manual analysis of tracing images. (B) Ghosh lab Sholl analysis of tracing images. (C) Bitmap analysis of tracing images. (D) Ghosh lab analysis of direct bitmap images. (E) Bitmap analysis of direct bitmap images. (F) Ghosh lab analysis of blank images subtracted from analysis of tracing images. (G) Bitmap analysis of blank images subtracted from analysis of tracing images. (H) Analysis using an edited version of the Ghosh lab code as described in the text. Curves represent mean intersection values ±SD.